Comparison of a CFD fire model against a ventilated fire experiment in an enclosure

Yunlong Liu[1], Alfred Moser[2] and Yehuda Sinai[3]

[1] CSIRO Fire Science and Technology Laboratory
PO Box 310 North Ryde, NSW 1670, Australia
Email: Yunlong.Liu@csiro.au

[2] Air and Climate Group, Department of Architecture
ETH-Zentrum, WET A5, CH-8092 Zurich
Swiss Federal Institute of Technology, Switzerland
Email: moser@hbt.arch.ethz.ch

[3] CFX Ltd., ANSYS CFX,
The Gemini Building, Fermi Avenue
Harwell International Business Centre
OX11 0QR United Kingdom

Abstract:

Computer modeling of fire has become an attracting approach for the fire safety assessment of proposed building structures. To devise and validate the fire model, a general-purpose computational fluid dynamics (CFD) software package, CFX, has been evaluated against a fire test case in a ventilated room. The test room is 6.0m long, 4.0m wide and 4.5m high with an exit opening of 0.65m x 0.65m. A simple inert fire model is used, in which a constant volumetric heat release is introduced at the location of the fire source to represent the fire. Combustion chemical reactions are not included in the computation, there was no flame spread and flashover to the wall lining material in this experiment, as the wall lining was non-combustible. The heat contribution is solely from the burner. It has been demonstrated that both the $k-\varepsilon$ model and the Shear Stress Transport (SST) hybrid turbulence model are capable of predicting the fire-generated turbulent flow and heat transfer. The computational result has an error of about 20 degree C when compared with the measured gas temperature of the Lawrence Livermore National Laboratory (LLNL), in which the heat release from a gas burner is used to represent a fire. It has been confirmed that the thermal energy deposit into the wall plays a significant role in the whole transient process. From the numerical point of view, the exterior wall thermal boundary condition treatment has little influence on the fire inside the room, as at 20 minutes after the start of the fire, heat penetrates only about 3 – 4 centimeters into the 20-cm-thick wall in this experimental case. The energy budget has been analyzed to understand the energy transfer for this fire test case. According to this test, about 30 percent of the heat from the fire is released by thermal radiation, and about 30 percent is carried out of the room by the ventilation air over the first 20 minutes after ignition, the rest is deposited into the walls, ceiling, and the floor.

It can be concluded that CFX can serve as a tool for the modeling of fire generated heat transfer in an enclosure. Thermal radiation plays an important role in the heat transfer process

from the fire. It has been concluded that, in order to accurately simulate a fire case, the conjugate heat transfer must be included in the fire mathematical model.

Key words: Fire, CFD model, transient, thermal radiation, conjugate heat transfer, turbulence.

Nomenclature:

ρ : Density (kg m^{-3})
λ : Conductivity (W m^{-1} K^{-1})
c_p: Heat capacity (J kg^{-1} K^{-1})
δ : Wall thickness (m)

y+: non-dimensional distance from the first near-wall grid node to the wall

1. Introduction

The research on fire spread has drawn more and more attentions worldwide, this is because accidental fire poses a great threat to human life and property. Architectural engineers must account for the fire risk and implement fire protection strategies during the early structural design stage to minimize losses. An accurate estimation of the fire-generated heat transfer and the evacuation time can serve as a good reference for engineers in the architectural design stage.

The performance of digital computer systems has greatly improved during the last decades. The computational fluid dynamics (CFD) modeling approach gained impetus in the fire science and technology because it is efficient and economical compared to the traditional experimental approach. Moreover, detailed information about the flow field and temperature distribution that are important to the fire spread mechanism becomes accessible by the CFD approach.

Several CFD software packages have been developed in the past years[1], some of them are specially designed for fire modeling, such as the Fire Dynamics Simulator (FDS) developed by the National Institute of Standard and Technology (NIST) in the USA, Smartfire[2] by Greenwich University in London, the UK. Furthermore, several general-purpose software packages are also good fire modeling tools, such as CFX[3] developed by ANSYS, FLUENT[4] developed by FLUENT Ltd, and PHOENICS[5] developed by CHAM.

However, CFD modeling of the fire test case involves several areas such as fluid dynamics, turbulence, heat and mass transfer, combustion, chemistry, mechanical systems, and structural properties of the enclosure. Thermal radiation plays an important role in the heat transfer process. Moreover, fire-generated turbulent buoyancy-driven flow dominates the fluid flow. Both the thermal radiation and buoyancy-generated turbulence had to be modeled when CFD was applied to this test case.

The objective of this investigation is to validate a fire model by a general-purpose CFD package, CFX, for the modeling of fire related heat transfer and smoke spread, and to identify

the factors that influence the mathematical modeling of a test fire. At present, it is not possible to account for all the details of a fire in the CFD modeling because a typical fire is extremely complicated. How to simplify the complicated physics of a fire in an enclosure, so that the major features of the fire are captured, is still an important issue of modern CFD modeling.

There have been many studies on the numerical simulation of fire in enclosures, in compartments, and in tunnels, and much progress has been made recently. Novozhilov[6] gave a comprehensive review of the latest developments.

Cox and Kumar[7], Lockwood and Malalasekera[8], and Yan[9] simplified the heat conduction inside the solid wall into a one-dimensional problem and take the thermal penetration depth as a known value. With these simplifications, the temperature field in the gas flow region inside the fire test room has been modeled successfully.

For the accurate modeling of the gas flow field, reliable turbulence models are required to model the buoyancy-generated turbulence. Large-Eddy Simulation (LES) is drawing the scientists' attention for the application in fire modeling[10-13]. It is more accurate for modeling the turbulent flow phenomena. The Fire Dynamics Simulator (FDS) is one of the codes built upon this concept. In the present study, the Lawrence Livermore National Laboratory (LLNL) fire test case has been simulated during the first 20 minutes of the fire using TRANS (Reynolds-Averaged Navier Stokes and Transient RANS)[14-15].

Solving the solid-wall heat conduction in conjugation with the thermal radiation and convective heat transfer at the wall surface is an approach which resides at the high end of the spectrum of complexity from the viewpoint of numerical modeling. In this approach, the computation domain extends to the exterior surface of the enclosure walls and ceiling. The inner wall surface temperature is automatically determined as a result of the heat exchange between the gas domain and the solid domain by CFD simulation of the conjugate heat transfer. At the exterior wall surface we only specify the heat transfer coefficient and the outdoor ambient air temperature. The balance between thermal radiation, heat convection, and heat conduction at the inner wall surface is satisfied automatically.

2. LLNL Experimental test

As an example of forced-ventilated fires in enclosures, Case MOD8 of the LLNL experiment by Alvares et al.[16] was chosen as the benchmark case. The room size is 6.0m long, 4.0m wide, and 4.5m high. The fire source is located on the floor center, with a constant heat release of 400 kW after the start of the fire. The displacement ventilation rate is $0.5m^3/s$, which is maintained by a fan located at the exit, and the ambient air temperature (outside of the enclosure walls) is 20°C. Figure 1 shows the geometry of the test model; the exit opening (65cm x 65cm) is on the vertical centerline of the west wall (4m x 4.5m high), with its center located 3.6m above the floor. The outdoor fresh air supply opening, which is made up of four equally-sized horizontally-distributed rectangles (0.5m long x 0.12m high), is located on the lower part of the south wall with the horizontal centerline 0.1m above the floor. These air supply rectangles were simplified into one horizontal rectangle (2m long x 0.12m high) in the CFD modeling.

At 20 minutes after the ignition of the burner, the ventilation rate and the temperature distribution along two key vertical lines on either side of the fire source, called east rake and west rake, and along the center vertical line in the south wall surface, have been recorded by

LLNL. These temperature profiles formed the basis for the validation of the fire model by the ANSYS-CFX software package in this investigation.

The walls and ceiling consist of a 10-cm thick Al_2O_3-S_1O_2 refractory. Table-1 is an overview of the physical properties of the enclosure.

TABLE 1: LLNL test wall structure information [16]

Property	Floor	Walls	Ceiling
Density ρ (kg m^{-3})	1440	1440	1920
Conductivity λ (W m^{-1} K^{-1})	0.39	0.39	0.63
Heat capacity c_p (J kg^{-1} K^{-1})	1000	1000	1000
Wall thickness δ (m)	0.5m	0.1m	0.1m
Emissivity	0.95	0.95	0.95

3. Numerical Details

The computation domain is made up of two parts: The fluid region and the conjugate-heat-conduction region with heat storage inside the walls, floor, and ceiling. The heat transport within the solid walls is modeled in three dimensions. Fire spread and combustion was not considered in this investigation. In the actual experiment the heat was generated by an iso-propanol flame positioned at the fire source location. In this study, the heat transfer coefficient from the exterior wall to the outside air is set at a value of 6W/m^2K. The airflow and heat transfer in the room and the heat conduction inside the wall are not sensitive to this parameter as will be discussed in the following section. The ceiling is treated in the same way as the walls except that the material is different. The computation domain on the floor is extended 0.5m deep into the ground and the temperature is set to 20˚C at a depth of 0.5 meters below the floor.

The fire source, which is the iso-propanol burner in the experiment, is simplified into a cylindrical volume heat source with a diameter of 0.28m and a height of 0.5m in the fluid region. This cylindrical volume heat source is situated 0.04cm above the floor to mathematically represent the LLNL situation. The total constant heat release rate after ignition is 400kW from this cylinder. No information is available about the growth of the heat release after ignition. In the CFD modeling a linear heat release from 0kW to 400kW was imposed for the first 30 seconds to represent the actual ignition situation. The heat generated by this heat source is transferred to the surrounding gas and the wall surfaces by thermal radiation, heat convection and conduction. Combustion was not included at the present stage of the research.

Total mesh size is about 200,000 cells. In the near-wall region, grid lines are arranged parallel to the surface, their mesh size was controlled at about 0.002m, which gives a y+ value of about 10-20, where $y^+ = \frac{y u_{tau}}{\nu}$ (u_{tau} is the shear stress velocity, y is the perpendicular distance from the wall surface to the first near-wall grid point center, ν is the kinematic viscosity). The

largest mesh size in the whole computation domain is 0.3m. The mesh within the walls, the ceiling and the floor has 21 parallel and elongated cells across the wall thickness.

The Shear Stress Transport (SST) turbulence model[17], developed by the ANSYS-CFX company, and the k–ε model were employed for resolving the turbulent buoyant flow. The SST model is a hybrid model, which incorporates the features of the k–ε and the k–ω models. In the near-solid region, where a laminar sub-layer exists, the low-level turbulence is modeled by the k–ω model as this model is more accurate for the near-wall treatment; in the region far from the wall, the k–ε model is employed for the modeling of the fully turbulent flow. In this study, both models have incorporated the buoyancy terms into the source terms of the governing equations.

The thermal radiation was treated by the Discrete Transfer (DT) radiation model[18-19], which can predict the radiant heat transfer with participating media. In the actual fire test case, the chemical species such as CO_2 and H_2O can influence the radiation heat transfer, as these species can absorb the radiation energy. In this CFD simulation the absorption coefficient[20] was chosen assuming the existence of CO_2 and H_2O to represent the actual fire test case, and it was assumed that there was no scattering of the radiation. As shown in the result of Figures 10 and 11, varied gas absorption coefficients[20] were tested from 0.01 m^{-1} to 0.25 m^{-1}.

To simulate the real test case, a preliminary run was made without any heat source in the domain to establish the ventilation flow field with the forced airflow at a constant temperature of 20˚C, corresponding to the experimental conditions before the fire is ignited. This result is later used as the initial flow field of the transient computation. The numerical computation is regarded as converged when all the normalized Root Mean Square (RMS) residuals fall below 10^{-6}.

A time step of 0.1 to 0.3 seconds is employed for the initial stage (first three minutes) because the temperature change is fast in the beginning. Later this time step can be increased up to 1 second, while the number of iterations per time step is always fixed at 3. Table 2 shows the detailed information about time step length and iteration numbers. To compute a case with a total physical time of 1200 seconds, about 100 hours of CPU time are required for an AMD Athlon processor with a Central Processing Unit (CPU) speed of 1900MHz.

Table 2: Time steps and solution procedure

Physical time	Time step length	Time step number	Iterations per step
0-60s	0.1s	600	3
60-120s	0.2s	300	3
120-180s	0.3s	200	3
180-1200s	1.0s	1020	3

4. Results and discussion

In this section, we will discuss the numerical simulation results over the 20 minutes after the start of the fire test and compare it with the LLNL experimental data. The CFD predicted

results shown in Figures 2-9 are obtained using the SST turbulence model, and thermal radiation is calculated using the Discrete Transfer (DT) radiation model with an absorption coefficient of $0.2m^{-1}$, this case is named as Case A, as shown in Table-3.

Figure 2 shows the history of the CFD calculated gas temperature at three monitor points in the gaseous domain. Monitor point 1 is located midway between the east wall and the fire source and 0.3m above the floor, monitor point 2 is located at 2.25m above the floor and about 0.01m away from the south wall vertical centerline, and point 3 is located at the gas exit. It shows that the gas temperature rose fast within the first three minutes after the fire started. After three minutes, the gas temperature increased almost linearly. This is why a smaller time step was taken in the initial minutes and a larger time step was used later.

Figure 3 shows the history of the CFD-calculated gas temperature rise along the east rake. This figure shows that the hot layer occupies more space in the room than the cold layer does. The temperature development in the first two minutes is much faster than that in the later stage.

The calculated particle tracing is shown in Figure 4. Some of the fresh air entering the room through the supply gets entrained by the fire plume and participates in the burning process. The gases generated by combustion change directions many times while traveling in the room. The gases from the fire source move up to the ceiling because of the buoyancy and later descend after hitting the ceiling. The hot gas exits the room through the extract by a fan, and this is why this case is called *ventilated fire test*.

Figure 5 shows the temperature field developing history within the room and inside the east wall. The x-coordinate is the east-west line extending from the center of the east wall: $-0.1<x<0$ refers to the solid wall domain, $0<x<0.1$ refers to the indoor gas domain, and the plane at $x = 0$ is the interface between the inner wall surface and indoor hot gas. According to Figure 5, the temperature field rise inside the wall is slower than that in the gas domain. The temperature rises much faster in the gaseous domain. This is because the thermal resistance in the solid is much higher than that in the gas domain. This also endorses an argument that the solid wall plays an important role in the whole heat transfer loop after the fire has started, and it is necessary to include the solid wall heat conduction and heat capacity into the computational domain.

According to Figure 5, the influence of the enclosure fire onto the wall results in a penetration depth of about 2-3cm at 20 minutes after the start of the fire, as confirmed by the LLNL experiments[16]. The remaining 7-8cm of the wall near the exterior surface stay at the initial temperature and are not affected by the fire in the room. This is due to the thermal inertia of the solid, which can be judged by the fact that a steep gradient in temperature is located in the wall near the wall-gas interface, but not in the air domain near the wall surface. Figure 5 also shows that the temperature of the exterior wall remains unchanged over the first 20 minutes after the fire started. This explains why the heat transfer coefficient value for the exterior wall surface has no influence on the heat and mass transfer inside the room in the first 20 minutes of the fire.

Figures 6 and 7 show the temperature field in two sections at Z=2m and X=3m, respectively. It is obvious that the temperature inside the wall is much lower than that in the indoor gas region. The upper zone of the room is about 100 degrees hotter than the lower zone.

Figure 8 shows the iso-surface of 230˚C air temperature within the room, which occupies about 30 percent of the room space. The hot gas buoyant flow generated by the fire formed a plume and rises to the ceiling. This picture gives a clear view of the two layers, the hot and cold layers. The numerical result shows that about 70 percent of the room space has an air temperature lower than 230˚C.

Figure 9 shows the flow field in the central section and the horizontal plane near the floor, from which a maximum velocity of about 3m/s to 4m/s can be found located immediately above the fire source.

Figure 10 presents the measured and CFD-predicted gas temperature profiles on the east rake, which is located mid-way between the fire source and the wall without gas exit fan. Figure 11 presents the measured and the CFD-predicted gas temperature profiles on the west rake, which is located mid-way between the fire source and the wall with gas exit fan. Table 3 explains the six variations that have been computed, the meaning of the legend in Figures 10 and 11 are also explained in Table 3.

Table 3: CFD fire models used in CFD modeling

Case no.	Symbol	Explanation of the physical meaning
Case 0	EXP	LLNL experimental result [16]
Case A	SSTradAbs02	SST turbulence model, DT radiation model is activated with an absorption coefficient of 0.2 m^{-1}
Case B	SSTnoradAbs02	SST turbulence model, radiation model is not activated, LLNL test heat source is imposed
Case C	SSTnorad60Abs02	SST turbulence model, radiation model is not activated, but take out 40 percent of the LLNL heat from the fire source
Case D	KEradAbs02	k– ε model, DT radiation model is activated with an absorption coefficient of 0.2 m^{-1}
Case E	SSTradAbs025	SST turbulence model, DT radiation model is activated with an absorption coefficient of 0.25 m^{-1}
Case F	SSTradAbs001	SST turbulence model, DT radiation model is activated with an absorption coefficient of 0.01 m^{-1}

Figures 10 and 11 demonstrate: The temperature profiles along the east rake and the west rake modeled by Case B (SSTnoradAbs02) and Case F (SSTradAbs001) both have very large errors when compared with the LLNL test result. In Case B, it is because the thermal radiation was not calculated, and all the heat release must be transferred by means of convection and conduction, so the CFD modeling result is about 100 °C higher than the gas temperature measured by LLNL. The high absorption coefficient in cases A, D, and E leads to higher radiation by the heat source volume and increases the portion of radiative heat release from the source. A smaller portion remains for convective heat release, and the air temperature in these cases is lower than in cases B and F. In Case F, even though the thermal radiation is calculated, an absorption coefficient of 0.01 m^{-1} is too low for this case where participative thermal radiation plays an important role. This shows that a radiation model with an unrealistic absorption coefficient cannot handle the thermal radiation correctly. In Case C (SSTnorad60Abs02), thermal radiation was also not activated but 40 percent of the heat had

been intentionally taken out from the fire source in the CFD fire model; this is based on the assumption that the radiation will account for 40 percent of the heat transfer. In Case C, the gas temperature profile obtained from the CFD modeling is quite close to that of the LLNL test, this supported the assumption that about 40 percent of the heat release from the fire source is transferred by thermal radiation. In Case A (SSTradAbs02) and Case D (KEradAbs02), thermal radiation is resolved using the DT radiation model with an absorption coefficient of $0.2m^{-1}$, the SST and the k–ε models are employed, respectively. In Case E (SSTradAbs025), thermal radiation is resolved using the DT radiation model with an absorption coefficient of $0.25m^{-1}$ and the SST model is used for turbulence modeling.

Comparison of the CFD-predicted gas temperature and the measured result shows that both the SST model and the k–ε model are capable of predicting the temperature field in the gas domain, the error is only about 20 °C when compared with the experimental measured gas temperature in the hot layer. It is very encouraging that both turbulence models with buoyancy terms can predict the temperature field along these two key vertical lines, as shown in Figures 10 and 11, if the gas absorption coefficient is fixed at 0.2 m^{-1}. In Case E with an increased absorption coefficient of 0.25 m^{-1} for the DT radiation model, the temperature profile is 10 degrees lower as compared to that of Case A, where an absorption coefficient of 0.2 m^{-1} is used, this again shows that the predicted gas temperature field is sensitive to the gas absorption coefficient.

It should be pointed out that, according to the CFD result obtained by Case A, where thermal radiation is resolved by the DT radiation model with a gas absorption coefficient of $0.2m^{-1}$, about 33 percent of the heat generated by the fire is released in form of thermal radiation. The rest is dissipated by convection and conduction. As compared to the fire model employed in Case C, where 40 percent of the heat was taken out from the LLNL fire source and the thermal radiation model is not activated, the CFD modeling temperature is slightly lower than the result obtained by Case A because too much radiated heat was subtracted. This supports the CFD result and shows that thermal radiation accounted for about 33 percent of the heat transfer from the fire source.

Figure 12 gives the comparison of the south wall temperature obtained for Case A. The trend of the temperature distribution is predicted, the difference between the CFD-predicted wall-surface temperature and the LLNL test results[12] is about 20 °C in most parts of the measurements, except that the temperature in the region between 3m to 4m from the floor differs by about 30 °C from the measured result.

According to Case A, the CFD modeling predicted an average exit gas temperature of 209˚C, which approaches the LLNL test measured gas temperature of 200˚C. It was calculated that 31 percent of the heat released from the fire source was carried out of the room by the hot combustion products. The remaining energy reaches the solid walls and ceiling. A breakdown of the energy transfer is shown in Table 4 for the CFD modeling result of Case A. The heat balance shows that the numerical result agrees with the experimental result fairly well.

Based on the comparison of the measured and predicted temperature in the gas domain and solid domain, it can be concluded that ANSYS-CFX can serve as a tool for the fire modeling. For the implementation of the fire model, the settings of Case A are recommended.

5. Conclusions

We can draw the following conclusions:

1. It has been calculated that in this test case, about 70 percent of the heat generated by the fire is deposited into the walls, ceiling and the floor, the rest 30 percent is carried out of the room by the exit gas. This showed that the wall heat conduction and deposit should not be ignored. Assumption of an adiabatic boundary condition at the inner wall surface or neglecting conjugate heat transfer can result in substantial errors of CFD simulations.

2. The transient features of a fire scenario must be captured by the CFD fire model. Both mesh size and the time step length should be suitable to resolve the transient behavior accurately and economically.

3. Radiation plays an important role in the heat transfer process. The participative radiation from the gaseous media is as important as the surface-to-surface thermal radiation. Total thermal radiation accounts for about 30 percent of the total heat released from the fire source in this test case.

4. The temperature distribution in the room, especially in the early stage of the fire, is not sensitive to the numerical treatment of the exterior wall surface. During the first twenty minutes of the fire event, the temperature wave only penetrates 3cm into the wall, leaving the exterior surface temperature of the 10-centimeter-thick wall unchanged. Therefore, the boundary condition at the exterior surface will not influence the CFD modeling result in the room, if the first 20 minutes heat transfer is of interests. This suggested that fixing a heat transfer coefficient for the exterior wall is a realistic boundary condition for simulating the enclosure fires.

5. The general-purpose CFD software package ANSYS-CFX can serve as a useful tool for the modeling of fire. Both the Shear Stress Transport (SST) turbulence model and the $k-\varepsilon$ model with the modified buoyancy term proved to be successful in this case, insofar as one can judge that from comparison with experimental data. Turbulence modeling is important as fire-generated buoyant flow is usually turbulent.

Acknowledgments

This project is financially supported by the Swiss Federal Institute of Technology, ETH, in Zurich, Switzerland, while cooperating with ANSYS-CFX at Harwell in the United Kingdom. Constructive discussions with Dr. Suresh Kumar of the Building Research Establishment at Watford, UK, and Dr. W. Malalasekera of Loughborough University, UK, are kindly acknowledged.

References

1. Olenick, Stephen M., and Carpenter, Douglas J., "An Updated International Survey of Computer Models for Fire and Smoke," SFPE Journal of Fire Protection Engineering, 13 (2), 2003, p. 87-110.

2. J Ewer, E R Galea, et al, An Intelligent CFD Based Fire Model, Journal of Fire Protection Engineering, V10(1), 1999, pp12-27.

3. Simcox S, Wilkes et al, “Computer Simulation of the Flows of Hot Gases from the Fires at King’s Cross Underground Station, Fire Safety Journal, V18, P49-73, 1992.

4. D. Barrero, B. Ozell and M. Reggio, On CFD and graphic animation for fire simulation, The Eleventh Annual Conference of the CFD Society of Canada, Vancouver, BC, May 2003.

5. Glynn DR, Eckford DC & Pope CW, Smoke concentrations and air temperatures generated by a fire on a train in a tunnel, The PHOENICS Journal of Computational Fluid Dynamics and its Applications, Vol. 9 No. 1, pp 157-168, 1996.

6. V. Novozhilov, Computational fluid dynamics modeling of compartment fires, Progress in Energy and Combustion Science V27 (2001), P661-666.

7. G. Cox, S. Kumar, Field modeling of fire in forced ventilated enclosures, Combustion Science and Technology, V52, PP7-23, 1987.

8. F.C. Lockwood, W.M. Malalasekera, Fire computation: the "flashover" phenomenon, 22nd International Symposium on combustion/The combustion institute, PP1319-1328, 1988.

9. Zhenhua Yan, Goran Holmstedt, CFD and experimental studies of room fire growth on wall lining materials, Fire Safety Journal, V27, PP201-238, 1996.

10. Brandeis J, Bergmann DJ, A numerical study of tunnel fires, Combustion Science and Technology, V35, PP133-155, 1983.

11. Wei Zhang, et al, Turbulence statistics in a fire room model by large eddy simulation, Fire Safety Journal, V37 P721-752, 2002.

12. H. Y. Wang, M. Coutin, J. M. Most, Large-eddy-simulation of buoyancy-driven fire propagation behind a pyrolysis zone along a vertical wall, Fire Safety Journal, V37, PP259-285, 2002.

13. Kevin B, McGrattan, et al, Fire Dynamics Simulator (FDS) Manual, Technical Reference Guide, 2002Ed.

14. Markatos, N. C., Malin, M.R., and Cox, G., Mathematical modeling of buoyancy-induced smoke flow in enclosures, International Journal of Heat and Mass transfer, V25, PP63-75, 1982.

15. Jorgen Carlsson, Fire Modelling Using CFD, An introduction for fire safety engineers, Report 5025, Department of Fire Safety Engineering, Lund Institute of Technology, 1999.

16. N. J. Alvares, K. L. Foote and P. J. Pagni, Force ventilated enclosure fires, Combustion Science and Technology, V39, PP55-81, 1984.

17. F. Menter, Two-equation eddy-viscosity turbulence models for engineering applications, AIAA Journal, V32, N8, PP269-289, 1994.

18. Lockwood F.C. & Shah N.G., "Discrete transfer radiation model" Proc. 18th Symposium (Int.) on Combustion, Combustion Institute, pp 1405-1413, 1981.

19. Robert Siegel, John R. Howell. Thermal radiation heat transfer, 4th ed., New York, 2002.

20. ASHRAE Handbook Fundamentals, ISBN 1-883413-45-1, 1997.

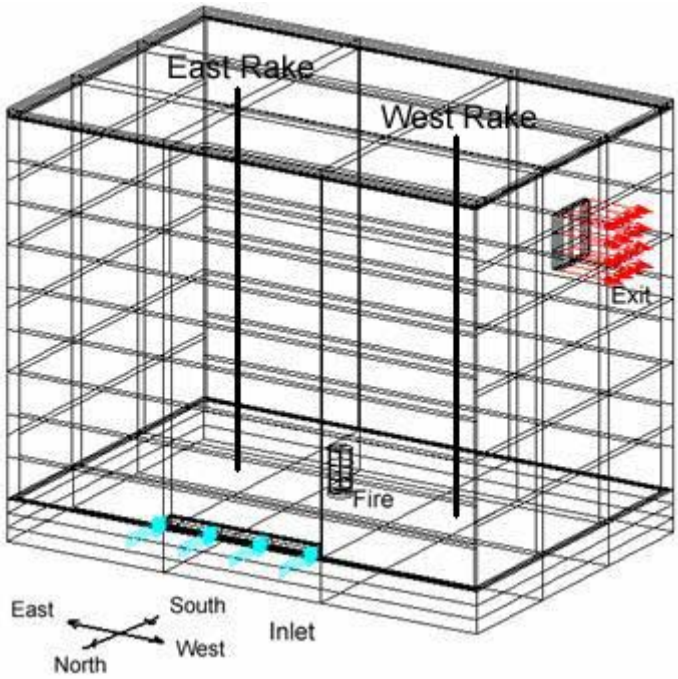

Figure 1: Schematic of the test room (LLNL[12], 1984)

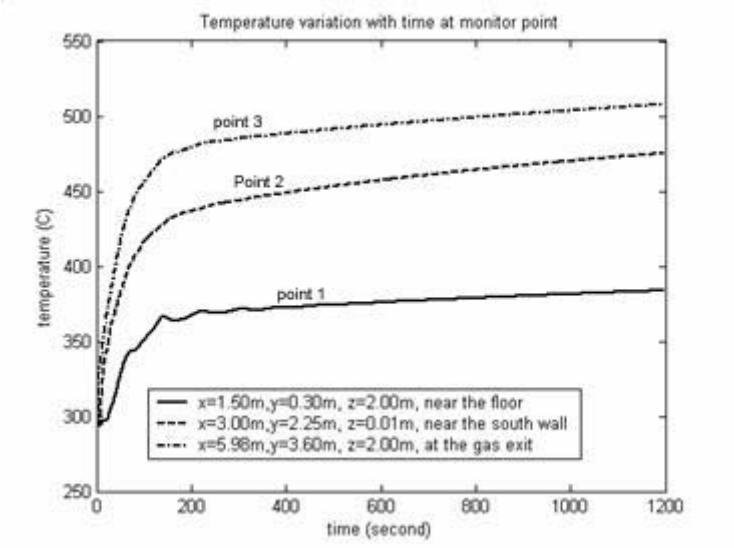

Figure 2: Temperature increase history after ignition at the monitor point 0.3m above the floor, 0.01m near the south wall, and at the gas exit.

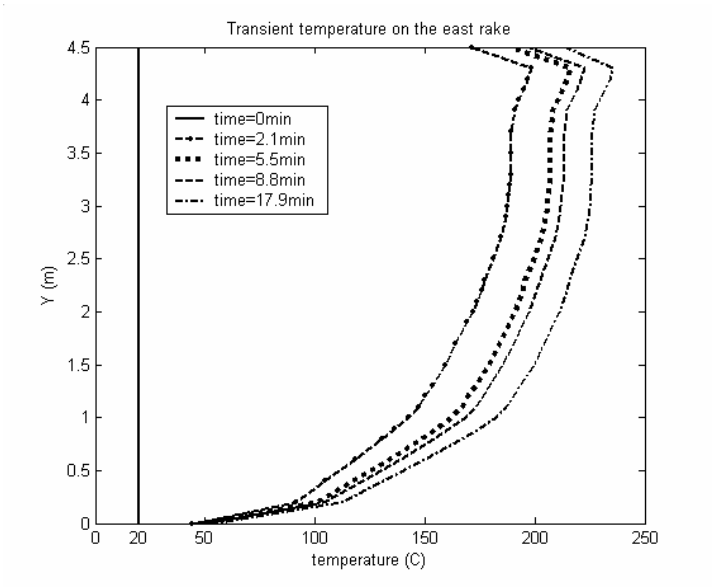

Figure 3: Transient temperature on the east rake

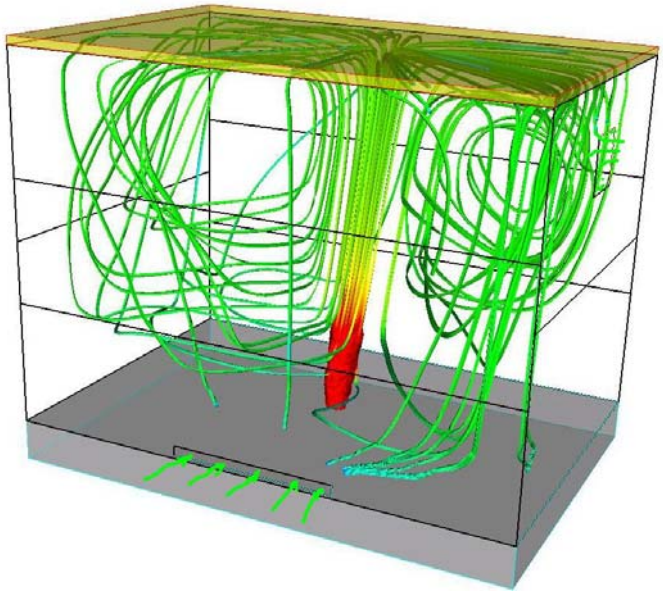

Figure 4: Streak lines starting at the fire location.

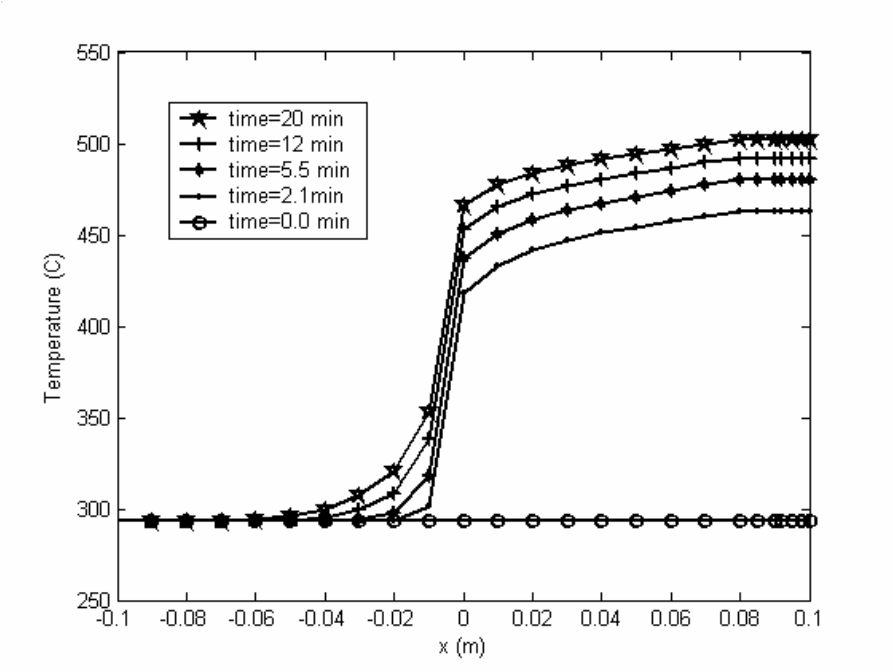

Figure 5: Temperature distribution along the East-West line (x) at the center point of the east wall and in the gas region near the surface (the points marked on the curves are not related to the mesh, just symbols to help identify the temperature distributions at different times)

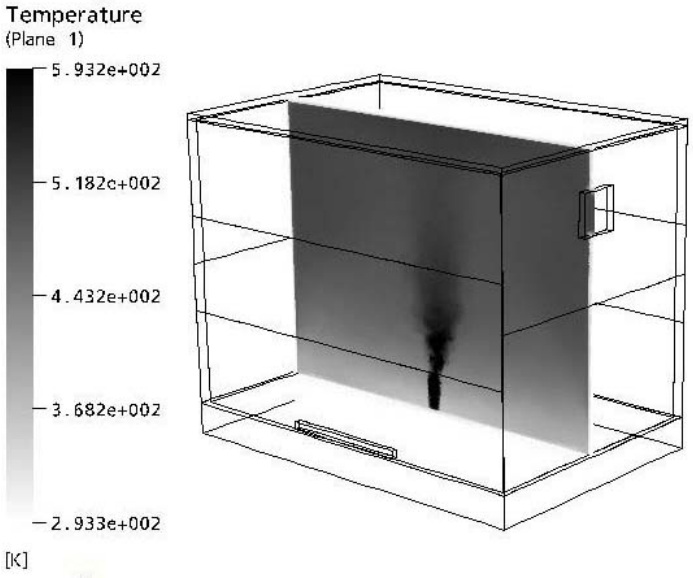

Figure 6: Temperature (K) field at section z = 2.0m and time = 20 min.

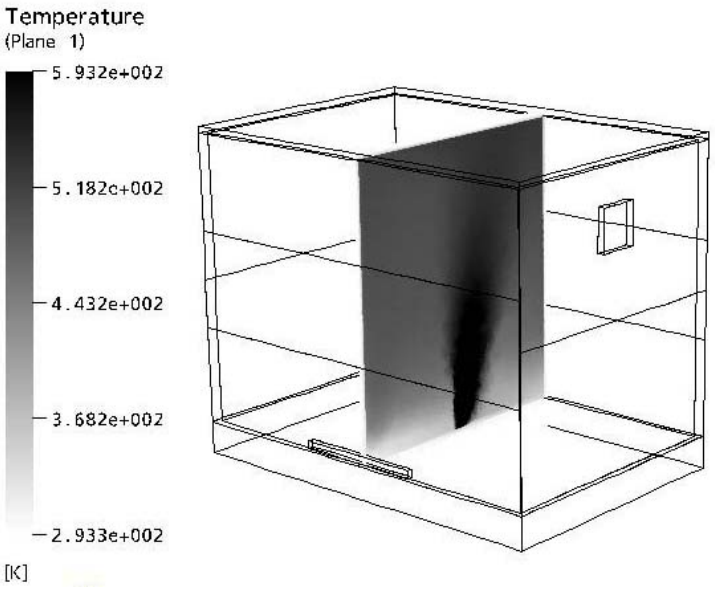

Figure 7: Temperature (K) field at section x = 3.0m and time = 20 min.

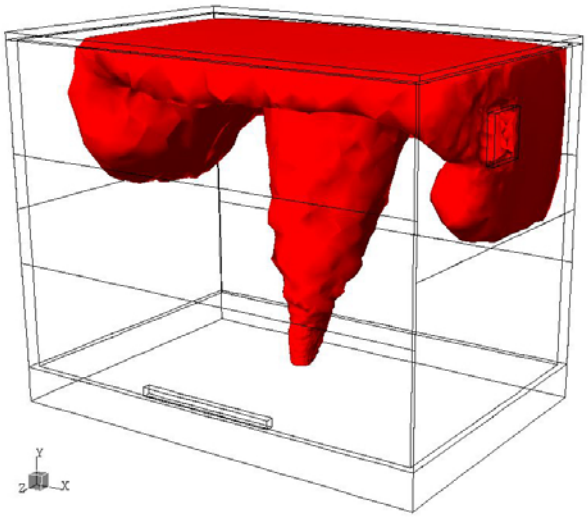

Figure 8: Iso-surface of gas temperature of 230˚C at time = 20 min.

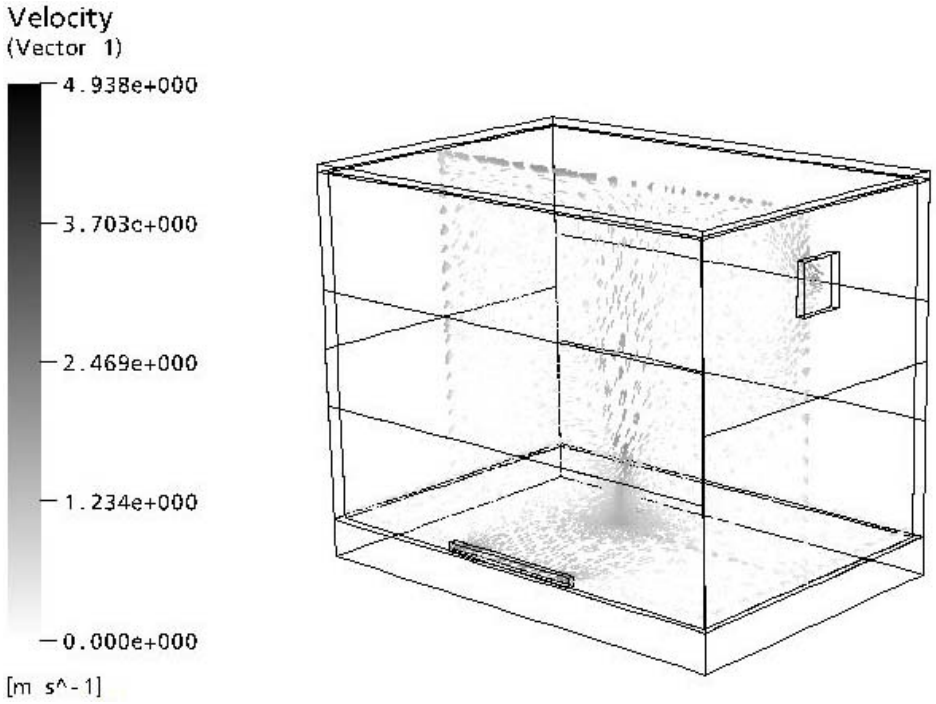

Figure 9: Flow field in the central plane and near the floor at time = 20 min.

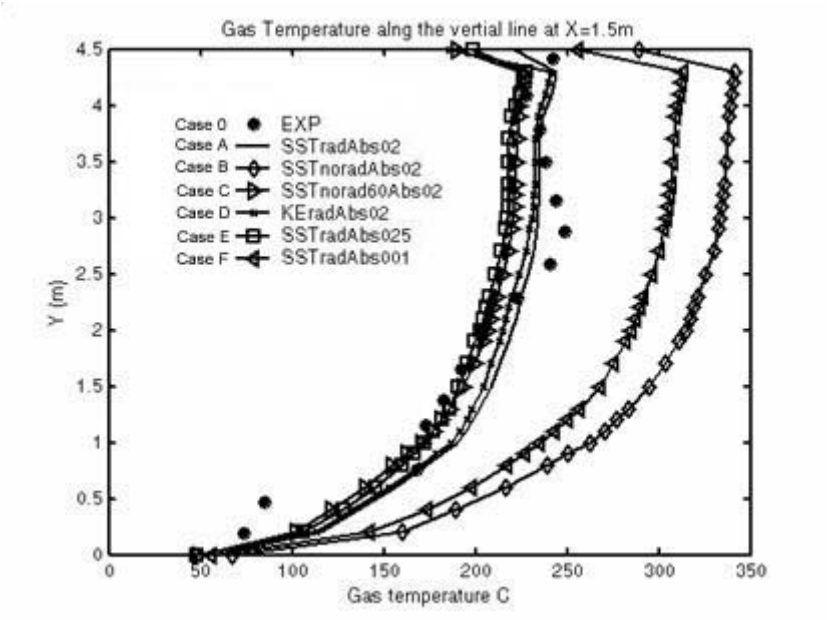

Fig 10: Temperature distribution along east rake at time = 20 min.

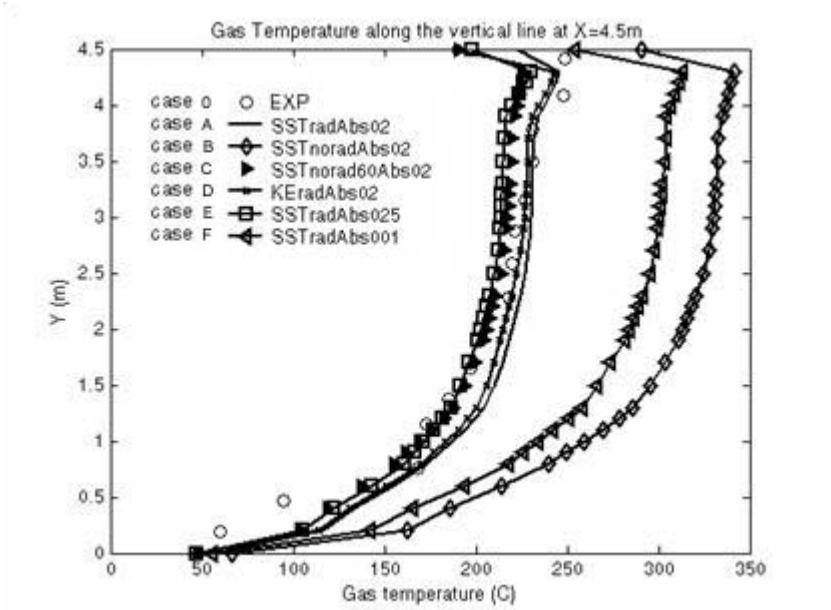

Fig 11: Temperature distribution along west rake at time = 20 min.

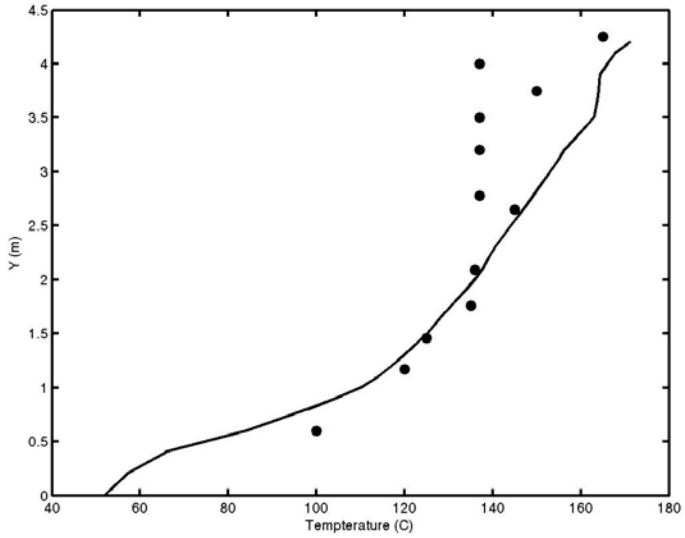

Fig 12: Temperature distribution vertically in the center of the south wall at time = 20 min.

Table 4: A breakdown of energy transfer in the computation domain

	Total	Gas Exit	Wall deposit
Numerical	400kW	124kW (31%)	276kW(69%)
LLNL test	400kW	108kW(27%)	292kW(73%)
Error	–	15%	5%